LUND UNIVERSITY
Faculty of Science

Optical FRAME: Investigating the effects of filtering the optical Fourier domain to be used as a new approach for FRAME

Sam Taylor

Thesis submitted for the degree Bachelor of Science

Project duration: 4 months

Supervised by: Elias Kristensson and Vassily Kornienko

Department of Physics
Division of Combustion Physics

June 2020

Acknowledgement

First and foremost I want to give my thanks to my supervisors, Elias Kristensson and Vassily Kornienko. To Elias, thank you for this opportunity to work in the lab, it has been one of the best and most rewarding experiences of my degree. Your patience when explaining concepts and your ability to do so with clarity helped with my understanding of these complex topics. To Vass, your endless enthusiasm and the countless hours spent discussing topics (work related or otherwise) was inspiring and encouraged me to continue working to strive for nothing short of my best. I cant thank you both enough for your time. To my family, friends, Juanita and many other loved ones, thank you for your encouragement and support during these times, it meant more than you realised and I hope to see you all soon. Finally, thank you to everyone in the Combustion Physics department and those in the lab who made my stay feel incredibly welcome! I wish you all nothing but the best in all your endeavours.

Abstract

Many important scientific phenomena require ultra-fast imaging to understand and investigate the characteristics of the event. Current methods of ultra-fast imaging that can obtain femtosecond time resolution rely on repeatable events or limiting the techniques versatility by completely remove the use of a dimension e.g. colour. FRAME is a novel technique which allows for ultra-fast imaging in the femtosecond regime for non-repeatable events without completely losing a dimension [1]. By superimposing a spatial modulation (tag) onto the illumination the beam of light can save information about an event. The tag is then decoded in post processing, thus gaining resolution in the tagged domain at the expense of the spatial resolution. In order to mitigate the spatial resolution reduction, this report present a new approach: Optical FRAME which performs the post-processing algorithm optically.

The new approach is demonstrated to have similar spatial resolution results to its digital counterpart, thus proving it as a standalone approach. Furthermore, Optical FRAME's unique property of retagging the beam can be utilised to optimise the spatial resolution of the setup. This report confirms that this unique property can be exploited and used to benefit the viability of FRAME. Retagging is here used to achieve temporally resolved imaging along with a doubled spatial resolution in the final images.

Contents

1 Introduction

Fundamental processes of the universe occur on timescales un-observable to the human eye. The development of ultra-fast imaging techniques therefore gives a unique perspective to investigate the world beyond our biological capabilities. Capturing dynamic events requires both the temporal and spatial data to be obtained from a single ultra fast event, thus there is need to develop ultra-fast imaging techniques that can be utilised in a broad range of experiments. Therefore, the information gathered from a single event must be organised in such a way to be able to separate the event's information according to a unique time stamp or tag to achieve ultra-fast imaging.

The information gained from the event is then carried by the photons and can be described using several different dimensions such as spatial (x,y,z), time (t) and colour (wavelength λ). The camera can only detect the (x,y) spatial dimensions in an exposure. However, trade-off's can occur between dimensions. Reducing or eliminating one dimension can be used to gain information and thus increase the resolution of another dimension. These trade-off's have allowed for current methods of ultra-fast videography such as STAMP (Sequentially timed all-optical mapping photography) which is able to capture single events with frame rates up to 1 THz [2]. The STAMP method utilises the dispersion properties of different wavelengths creating ultra short time gaps to image a single event. Each wavelength now carries the information for a specific time interval which can be separated to gain information about the event at a specific time. This removes the colour dimension (λ) but increases the temporal resolution drastically. STAMP, however, loses the ability to communicate in colour with the event and thus the use is limited. For ultra-fast imaging to be widely utilised, there must be a technique which has the flexibility to work in more arbitrary conditions without limiting the versatility or effectiveness of the technique.

Frequency Recognition Algorithm for Multiple Exposures (FRAME) is a tagging and deciphering technique that works by manipulating the spatial dimension of the illuminating beam [1].

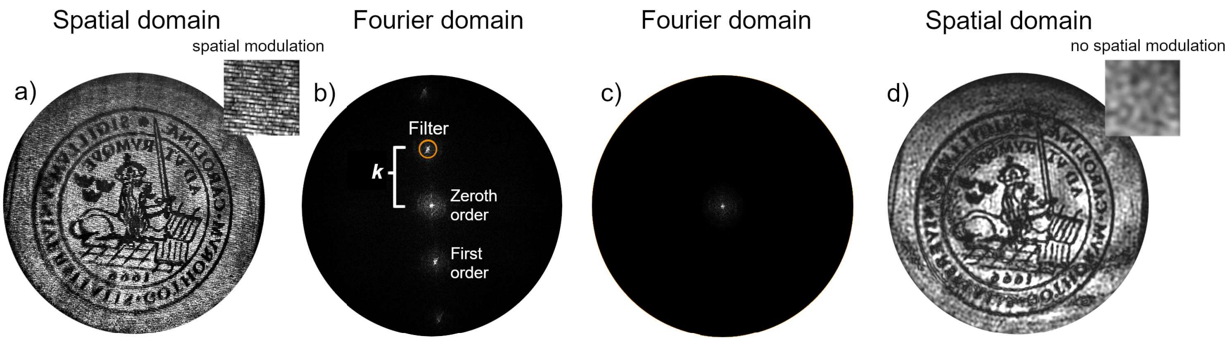

Figure 1: Operating principal of FRAME. **(a)** Image with spatial modulation creates "copies" of the image in the Fourier domain **(b)** each copy fills a small portion of the Fourier domain. A filter is applied to a copied image **(c)** which is transformed into the spatial domain now without the spatial modulation **(d)**

The approach works by superimposing spatial modulations onto the illumination such that the events information is tagged and encoded onto the beam. An example of the spatial modulation encoded onto the illumination can be see in figure 1. The spatial modulation acts as a tag which can be deciphered in post-processing. Once it is decoded using a frequency recognition algorithm, the image corresponding to the spatial modulation is obtained. For example, in 3D reconstruction, the image property of interest is the depth axis. Therefore, various spatial modulations tag several beams, each imaging the sample at different depths [1]. In one exposure the camera detects all of the beams encoded with different spatial modulations. Identifying and deciphering these tags identifies each beam and thus produces images with the information regarding the event at different depths. The same fundamental process can be applied to the temporal and colour dimensions for videography and multi-spectral imaging [1]

While this method reduces the resolution in the spatial domain as seen in figure 1 a) - d), it has the possibility to increase the temporal resolution to 200 femtoseconds [1] or 5 THz. As FRAME can illuminate samples at arbitrary wavelengths it can, for instance, gain the colour dimension (λ) and be used for spectroscopic measurements thus adding to its flexibility.

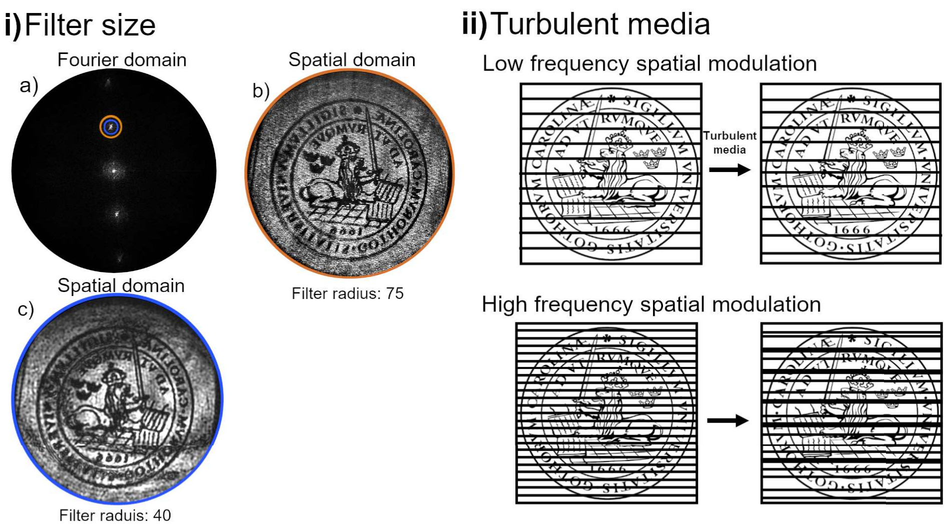

Figure 2: i) Filter size: The size of the filter impact the resolution of the image. **(b)** is of higher resolution than **(c)**. **ii) Turbulent media:** Two different spatial modulations with varying frequency passing through a turbulent media. The higher frequency spatial modulations attenuate higher than the lower frequency counterpart.

The resolution increase in the desired dimension is a result of a loss in spatial resolution. This trade-off occurs due to filters applied to the frequency domain (referred to as the Fourier domain). The size of the filter in the Fourier domain determines the resolution in the spatial dimension as shown in figure 2 **i)**. Smaller filters are required if the Fourier points are clustered close together, thus reducing the spatial resolution. To reduce the loss of spatial resolution in the final images, higher spatial modulation can be encoded onto the illumination, increasing the distance between Fourier domain points. This allows a larger filter to be passed over the Fourier points, reducing the loss in spatial resolution. However, high spatial modulations are much more sensitive to turbulent samples or environments with vibrations as shown in figure 2 **ii)**, attenuating higher frequencies and thus reducing the image quality. For such samples a trade-off exists between the image quality and the spatial resolution. Therefore, the use of FRAME is restricted to samples of lower turbulence.

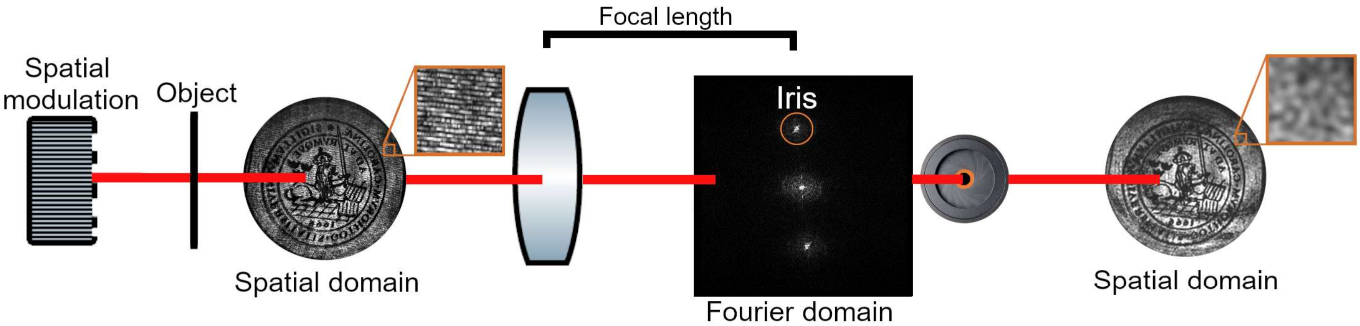

Figure 3: The spatial modulation encoded into the beam can be seen in the Fourier domain of the optical setup. By cutting the image copy with an iris the copy of the image can be obtained.

While FRAME currently accesses and manipulates the Fourier domain using post-processing techniques, it is not the only way to access the Fourier domain. A similar method of FRAME can be performed optically as shown in figure 1. The Fourier domain of a beam of light can be found at the effective focal length of the lens (derivation shown in appendix C.2). By knowing the spatial frequency mapping of the optical Fourier domain, it is possible to isolate the Fourier domain points, similar to the filters performed digitally. This opens up a possibility to perform FRAME faster than its digital counterpart with the potential to reduce the aforementioned trade-off issues. The following report compares digital and optical FRAME and investigates the usefulness of optical FRAME.

2 Background

The background section covers concepts that are needed to understand and discuss the mechanisms behind both optical and digital FRAME.

2.1 Camera optics

An imaging systems performance can be measured by the resolution of the final image. The measurement of an image's resolution is often called its spatial resolution and is defined as the ability to distinguish between two closely aligned points sources, often generalised to closely aligned lines as shown in figure 4 **i)**. The green line refers to a point beyond which the lines can no longer be resolved. This give a generalised way to compare different imaging systems. However, there are two distinct components which limit the spatial resolution: The optical resolution of the setup and the number of pixels in the sensor.

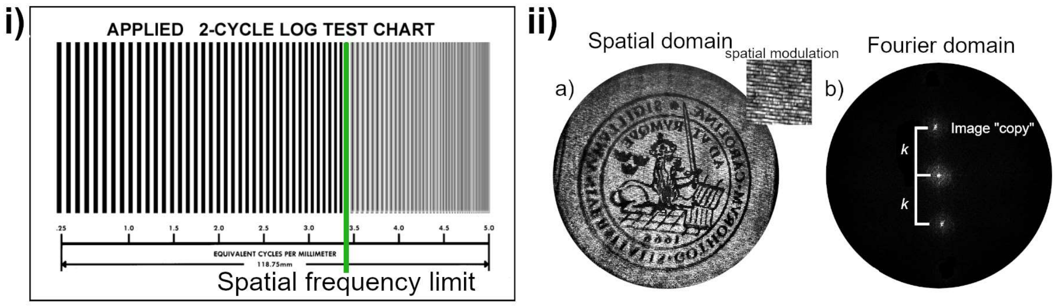

Figure 4: i) Figure adapted from [3]. A wide variety of different spatial frequencies. These spatial frequencies can be distinguished until a specific value defined as the spatial frequency limit. This method is used to quantifying the spatial resolution of an image. **ii)** a An image with a spatial modulation (due to the Ronchi Grating) is Fourier transformed such that the image b) has two image "copies" at distance k from the zeroth order

While most have an understanding of a camera's function, specific definitions relating to a camera's pixel count may be important to be able to differentiate the limiting factors to an image's spatial resolution. The amount of detail that the image sensor can potentially capture is limited by its pixel count. The higher the number of pixels the greater the image's potential spatial resolution. Another way of conceptualising this is an increase in an image sensor's pixel count increases the amount of information that an image can hold which in turn can, but not necessarily, increase its resolution.

The optical resolution of the setup describes the capability of the system to resolves details about the object being imaged. In this thesis the camera's pixel count is fixed such that the setup defines the spatial resolution limit of the image. Reduction in optical resolution occurs as apparatus like lenses and irises spatially constrain the beam by discarding higher spatial frequencies and thus reducing the spatial resolution of the image. However, by knowing the spatial frequency mapping of the beam it is possible to isolate specific spatial frequencies. This is important when trying to decode tags which use the spatial dimension such as the spatial modulations.

2.2 Optics: Tagging

Tagging light involves manipulating a dimension of a beam to make the designated dimension detectable in a later stage of the setup. Cameras can only detect the x and y spatial dimensions. However, as previously mentioned photons carry much more information than the camera is detecting. The information carried by a photon can be described in nine dimensions (x, y, z, θ, ϕ, λ, t, Φ, χ), these are the spatial coordinates (x,y,z), the propagation polar angles (θ, ϕ), the wavelength (λ), emissions time (t), the polarisation orientation (Φ) and the ellipticity angle (χ) [4]. Each dimension can be thought of as possible ways to tag a photon. By interacting with these tags it is possible to detect characteristics of the 9 dimensions of the beam rather than the 2 dimensions that the camera detects. To do this without the use of specific apparatus (e.g. polarisation camera), the spatial dimension can be tagged and exchanged to increase the resolution of another dimension. This trade-off between dimensions is vital for how FRAME operates. For this process to work, a spatial tag is created to artificially tag another dimension. A method of applying this spatial modulation is with the use of a diffraction grating (Ronchi grating).

A diffraction grating is an optical object defined by its periodic changes of transparency, between opaque and translucent bands. This periodicity can be described by a specific spatial frequency or wave vector k. As diffraction is a wave based phenomena, it is useful to describe the beam of light as a wave-front with a corresponding wave vector in each spatial dimension $k = (k_x, k_y, k_z)$. The diffraction filters' spatial frequencies are perpendicular to the direction of travel of the beam. Therefore, light waves passing through the diffraction grating gain an addition wave vector perpendicular to the direction of travel. The magnitude of the additional wave vector is due to constructive and deconstructive interference occurring at distinct angles described by the condition for constructive interference: nλ = sinθ d. Light that passes with no additional wave vector is known as the zeroth order while the first angle where constructive interference occurs, and thus having an addition wave vector, is known as the first order. The diffraction grating provides several unique wave vectors to the beam, meaning to fully describe the diffraction grating's spatial frequency and therefore its image, one must recombine all orders. Note that while higher orders than the first order exist they are ignored for this thesis as their role is insignificant.

If instead the beam passing through the diffraction grating contains an image, each order contains a "copy" of the original image as shown in figure 4 **ii)**. The challenge then becomes isolating this "copy". As previously described, the additional spatial frequency k vector from the diffraction grating is added to the wavefront resulting in the first order beam. Therefore to isolate the first order beam one must access the frequency domain and identify this additional k vector.

This thesis examines two distinct methods of accessing the frequency domain, otherwise known as the Fourier domain: Through optical manipulation and through software analysis. These are the two main distinction between optical and digital FRAME.

2.3 Fourier domain

2.3.1 Fourier Transform

Before gaining access to the Fourier domain, it is important to understand how the domain operates and its dimensions. One way of accessing the Fourier domain requires a mathematical transform between the spatial domain (x,y) and the spatial frequency domain (Fourier domain).

The fundamental concept of the Fourier transforms is the Fourier theorem, stating that any periodic wave function can be expressed as an infinite sum of sinusoidal waves. Images can also be expressed as a sum of spatial sinusoidal function of certain frequencies. Each of these frequencies combine in the spatial domain to form the image, however in the Fourier domain the sinusoidal frequency amplitude are mapped instead. The dimensions therefore change from the spatial (x,y) dimension into the frequency (u,v) dimension. The frequency dimension has units of inverse length and the mapping expressed as an image as shown in figure 5 **i)**.

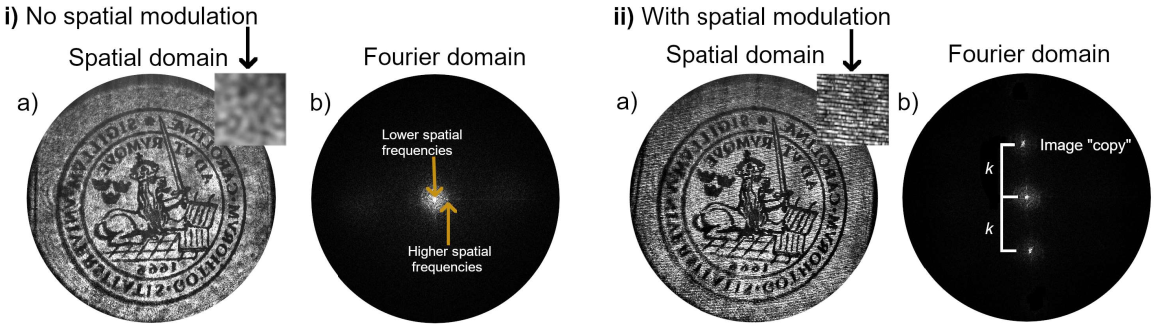

Figure 5: i) No spatial modulation: Spatial image **(a)** transformed into its Fourier domain **(b)**.
ii) With spatial modulation: The Fourier transformed image **b)** now has two additional image "copies" at a distance k from the centre Fourier point

The symmetry of the Fourier domain is also shown in figure 5 **ii)**. This is due to the symmetry in the diffraction gratings k vector. Every grating produces two first orders both with the same k but with an opposite sign. This translates to the Fourier domain such that the Fourier transform satisfies $|\mathcal{F}(u,v)| = |\mathcal{F}(-u,-v)|$. Hence both frequencies (u,v) and $(-u,-v)$ are treated the same, creating the symmetry. Thus it becomes clear how to understand the spatial frequencies of an image are distributed in the Fourier domain. Higher frequencies are mapped further from the centre of the Fourier domain while lower frequencies are closer to the centre. This distribution, however, is the basis for Fourier optics and becomes of utmost importance when manipulating the Fourier domain.

2.3.2 Accessing the Optical Fourier domain

Through Fraunhofer diffraction the Fourier domain can occur in the far field of a beam. The mathematical description behind this transformation is demonstrated in appendix B. However, to practically obtain this result requires a large optical setup. An easier method of accessing the Fourier domain utilises convergent lenses to bring the Fourier domain to the focal point of the lens [5]. At the focal point of the lens the wave fronts become parallel due to phase cancellation similar to the phase cancellation occurring in Fraunhofer diffraction. Therefore when doing a cross sectional projection of the focal point, the parallel wave fronts produce the Fourier domain. This phase cancellation is achieved as the lens' geometry and refractive properties obtain the Fourier transform (occurs in equation 9 in appendix B), removing the need for the Fraunhoufer approximation. For a more in-depth description of how lenses act as a Fourier transform the reader is refered to the Fundementals of Photonics book [6]. The location of the optical Fourier domain can be resolved using both the lens equation derived in appendix C.1 as well as the effective focal length of the system derived in appendix C.2.

Allowing the beam to propagate past the optical Fourier domain generates the inverse Fourier transform, returning to the spatial domain to be imaged. This gives an understanding of the spatial and Fourier domain locations in the optical setup. This knowledge is key to manipulating the spatial frequencies allowing optical FRAME to be achieved.

2.3.3 Spatial filtering

Spatial filters take advantage of the previously described spatial frequency distribution in the Fourier domain to remove or isolate specific frequencies. The spatial frequency mapping and isolation process can be examined in figure 1. Each Fourier point contains the "copy" of the image while the location of the Fourier point is the result of the additional k vector from the diffraction grating, otherwise known as a spatial frequency tag.

As the locations in the Fourier domain are distinct they can be isolated using a spatial filter (such as an iris or a mirror). However, isolating a point may remove higher frequencies that are outside of the spatial filtering mechanism thus acting as a low-pass filter and reducing the spatial resolution of the image. By increasing the distance between the Fourier points (k in figure 1) the size of the spatial filter can be increased to include higher spatial frequencies. To achieve the maximum spatial resolution, the spatial frequency tag must be sufficiently high to increase the distance between the Fourier points and allow for a large filtering mechanism. The previous sections describe an approach to optically tag, detect and isolate the image "copy" in the Fourier domain, obtaining the image all without the need for any post-processing. The resultant beam can be imaged and optical FRAME accomplished.

2.3.4 Digital Filtering

The fundamental concepts described above can be translated to the digital Fourier domain. Accessing the digital Fourier domain relies on using the mathematical Fourier transform equations for spatial frequencies. Digital filters remove parts of the Fourier domain image to manipulate the frequencies. The inverse Fourier transform equations can transform the image back into the spatial domain. This process can be observed in figure 1 where the transformation between each step is done digitally.

This gives a complete understanding of how to access and manipulate spatial frequency in both the optical and digital Fourier domain which will be utilised throughout this thesis.

3 Method

The project is divided into three parts in order to fully describe and understand the optical FRAME approach. Initially, a comparison between optical FRAME and digital FRAME is performed and the relative optical resolution tested. To further utilise optical FRAME in similar circumstances to digital FRAME, the setup is scaled up to accommodate multiple tags. Finally, investigation into the unique properties of optical FRAME is performed which may prove useful in future endeavours.

It is important to note that for the following experiments the laser used is a monochromatic HeNe laser with a Gaussian beam profile. The beam is enlarged by 5x and collimated to fully illuminate the samples and minimise beam divergence effects that may occur from the setup.

3.1 Optical Filtering vs. Digital Filtering

In order to test the spatial resolution characteristics of optical filtering vs digital filtering the Fourier domain of each approach is investigated. The differences between the two approaches are illustrated below.

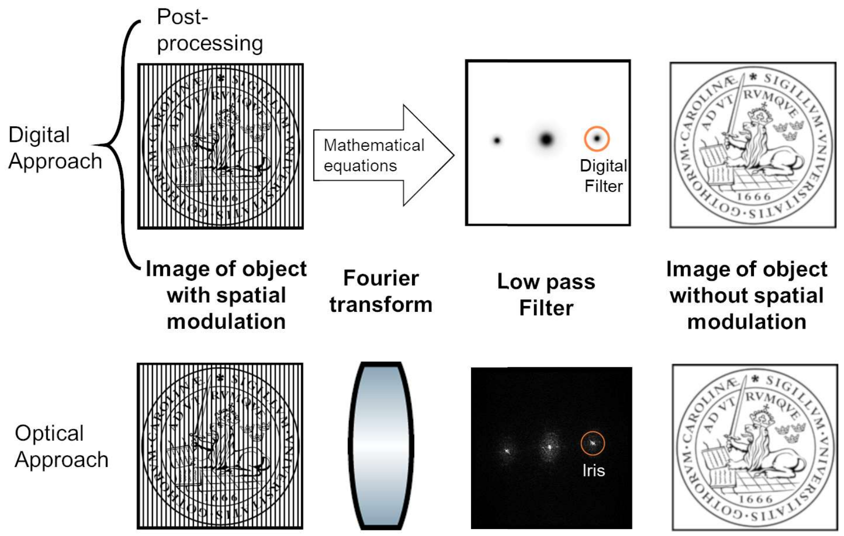

Figure 6: Optical and Digital filtering illustrated above. The post-processing requires mathematical equations to access the Fourier domain where it is manipulated by digital filters. The optical approach uses a lens to access the Fourier domain where it can be manipulated by an iris or similar filters.

To compare these approaches, it is important to understand how each approach handles spatial frequencies. By examining the final images spatial resolution, the optical resolution for each approach's method can be obtained and contrasted. One method of quantifying the spatial resolution of an image is by measuring the image's spatial frequency limit. The spatial frequency limit of an image is the value where the spatial frequencies lower than the limit can be distinguished but higher frequency can not. This is an important distinction for quantifying and comparing the spatial resolution of images. To obtain the spatial frequency limit and therefore measure the spatial resolution, an application is used to obtain the modulation transfer function (MTF) values for the image [7]. The MTF is a measurement of the setup's ability to transfer contrast at a particular spatial frequency from the object of the setup to the final image, including any post-processing that occurs. An example of this is demonstrated in figure 7.

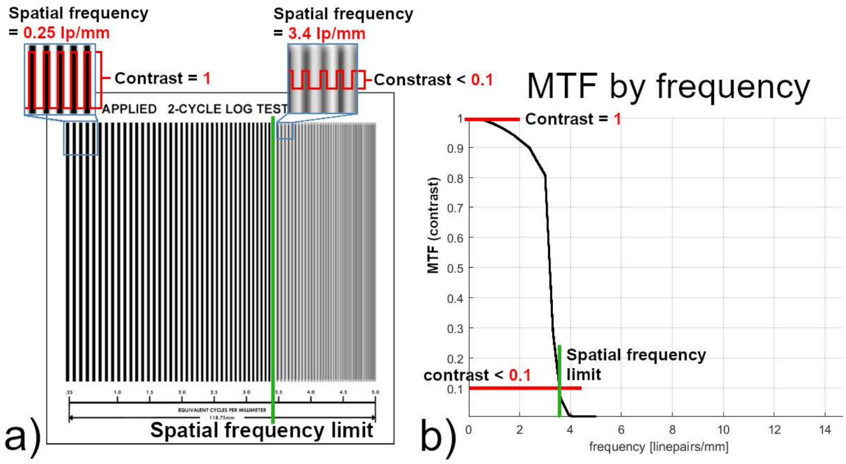

Figure 7: a) The image is analysed to obtain the contrast for each spatial frequency and is plotted in figure b). By establishing a contrast threshold, the image's spatial frequency limit can be calculated

In figure 7 a), the image is made up of a wide variety of different spatial frequencies, represented by the change in spacing between the lines. At a low spatial frequency the lines can be resolved as there is a high contrast between the black lines and the white background. As the spatial frequency increases, the ability to resolve the lines diminishes. By establishing a threshold contrast the image can be defined by the spatial frequency limit, or where the spatial frequency's contrast drops below the threshold as shown in figure 7 b). For this experiment the image that is used is a spiral target which also contains a wide variety of spatial frequencies as seen below.

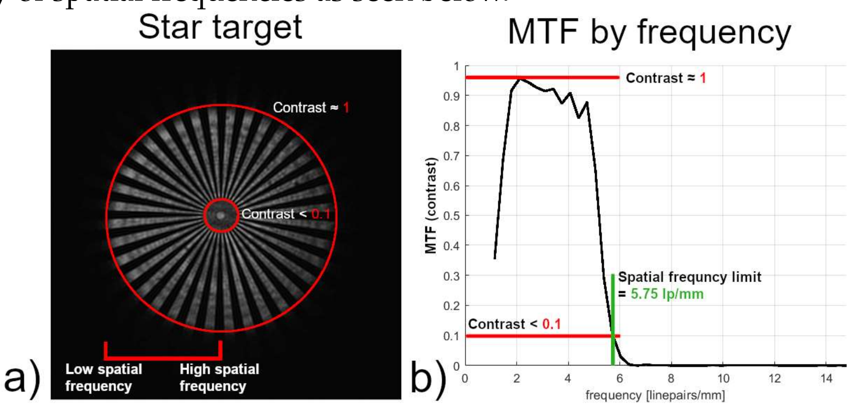

Figure 8: The final image of the star target a) is captured by a camera were it is analysed in a similar process as figure 7. Thus the spatial frequency limit of the image can be calculated

This star target shown in figure 8 a) is used throughout the experiments as a comparison tool. The previous analyses can now occur with the spiral target, with the chosen contrast threshold of 0.1. This reduced the fluctuations in the spatial frequency limit when changing low pass filter's radius. These fluctuations caused inconsistent drops in spatial frequency contrast at specific frequencies. Choosing a lower threshold value of 0.1 bypassed these issues while still keeping the sharp contrast of the MTF by frequency graph.

Now that the optical resolution can be quantified, there are two important factors to consider when comparing the approaches: How the setup handles the spatial frequencies and the size of the filter used when isolating a Fourier point. As previously mentioned, the size of the filter in the Fourier domain has a direct impact on the final image's spatial resolution which in turn changes the spatial frequency limit. Thus it becomes possible to understand how each approach handles spatial frequencies by varying the filter size in the Fourier domain and calculating the image's spatial frequency limit. To increase reliability of the comparison, the data for the two approaches are collected from the same setup, with the Fourier domain for each approach accessible. The diagram of the setup with these requirements is located at the end of this section.

However, as the optical low-pass filter radius is difficult to measure without specific equipment, another method is utilised. Assuming that the beam is passing through the centre of the iris (which is optimal), the intensity of the beam is proportional to the radius squared of the filter. Instead of measuring the radius of the digital and optical filters, the intensity of the filtered Fourier domain will be measured. The normalised image intensity for each approach can then be compared. After the filter is applied the image is transformed back into the spatial domain for further analysis. However, the approaches differ on how the filters are applied as shown by figure 6, as well as how the image intensities are obtained. These distinctions are further discussed in the sections below.

3.1.1 Digital Approach

From the setup, only a reference image is required for analysis as the digital approach relies on post-processing to execute FRAME. The processed reference image produces filtered images such that the intensity value and the spatial frequency limit can be extracted to understand how the digital approach handles spatial frequencies.

To obtain these values the reference image is run through the post processing method. By taking the Fourier transform of the star target a filter can be applied. Before transforming back to the spatial domain, the sum of the absolute pixel value in the Fourier domain is calculated giving the intensity value for the image. As the filter radius is only limited by the image's dimensions, different filters can be applied thus the final images have wide variety of spatial resolutions and intensities. Each image is then passed through the MTF application to obtain its spatial frequency limit. This value is saved along with the normalised intensity value. This process was achieved using an automated code, illustrated in appendix A.

3.1.2 Optical Approach

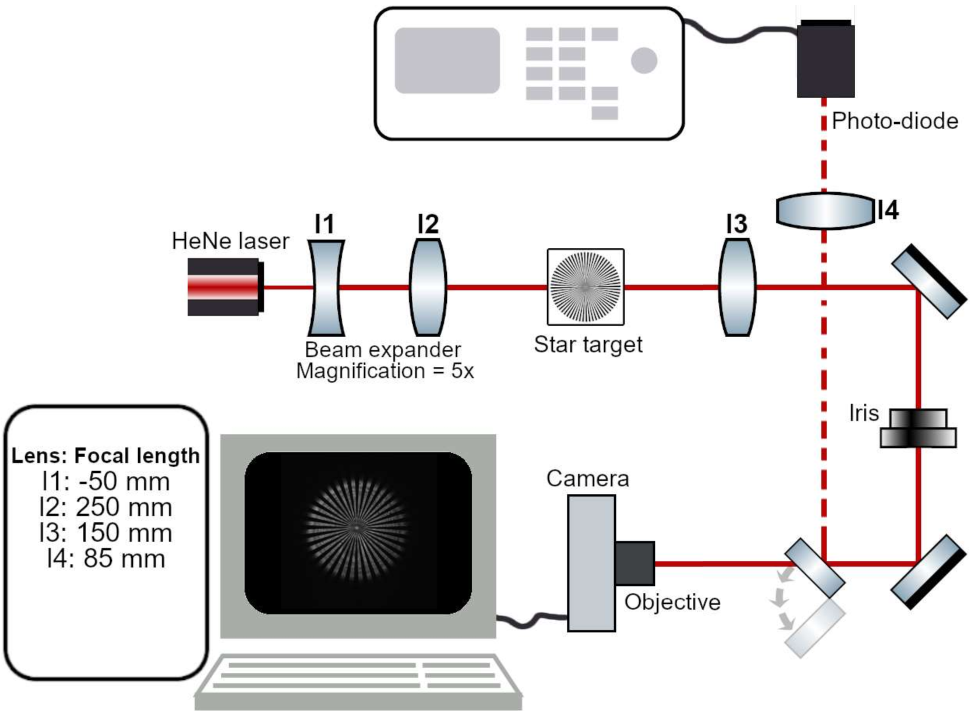

Figure 9: The Schematic of the setup shows the beam illuminating the star target after which a lens is used to access the optical Fourier domain, where the frequencies can be isolated using an iris. The final image can then be captured by a 1MP Andor camera equipped with an objective lens. This schematic is used for the optical vs digital comparison.

The post processing method described in the digital approach is accomplished here optically. In the setup shown in figure 9 the optical Fourier domain is surrounded by an iris. Adjusting the iris' radius changes the intensity of the beam, measured by a photo-diode. As previously discussed, applying an iris in the Fourier domain acts as a low-pass filter, thus reducing the spatial resolution of the image. The intensity of the Fourier domain is measured by a secondary lens focusing the beam onto the photo-diode while the spatial resolution is measured by the MTF application [7] as previously described. The direction of the beam to the photo-diode or camera is controlled by a flip mirror. Thus both the image and the intensity can be obtained optically at around the same time. The intensity is normalised by the intensity corresponding to the fully open iris.

To obtain the spatial frequency limit of the setup the MTF application is used similar to the digital approach. Thus, both the spatial frequency limit and the intensity can be collected for the optical approach.

3.2 Optical FRAME: Simultaneous tagging

In order to demonstrate that optical FRAME can be performed in similar circumstances to digital FRAME, one must show that the first order Fourier points in the optical Fourier domain can be isolated effectively. As such, two different objects are tagged with a unique spatial modulation. The setup shown in figure 10 isolates a first order using an iris located in the beam's Fourier domain.

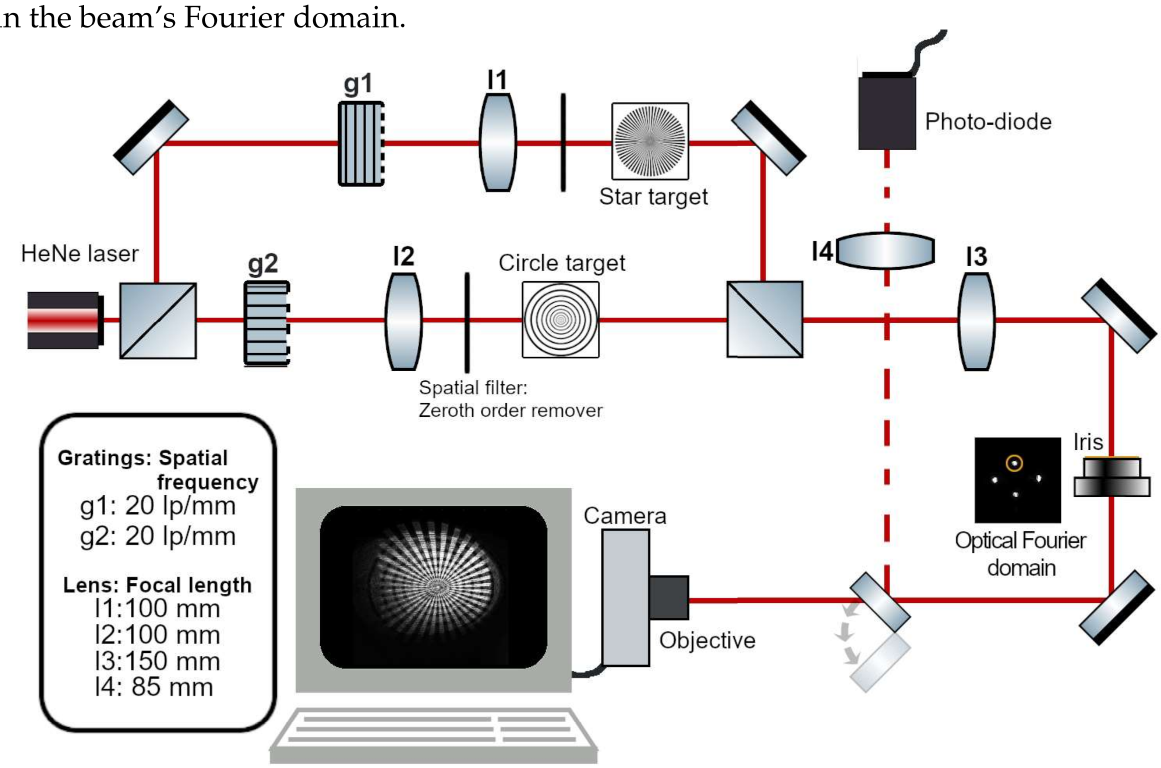

Figure 10: Schematics of the setup used for simultaneous tagging for optical FRAME. The setup is similar to figure 9 with the exception that the tag (grating) is also illuminated by the beam. To obtain multiple tags, a beam splitter is used to create another arm of the setup such that it can be tagged with a different grating. The Fourier point of interest is then isolated using a iris located in the optical Fourier domain. The final image is captured on a camera for spatial resolution analysis.

Varying the iris' radius gives the intensity and spatial frequency limit values used to measure the approaches optical resolution as described in the previous experiment. To show that the isolation is effective one must demonstrate that there are a negligible amount spatial frequencies from other order leaking through the iris. This is achieved by repeating the experiment and removing other orders via spatial filters in previous optical Fourier domains.

The final data from the experiment is then compared with the previous experiment to understand how the shape of the graph is impacted when utilising multiple tags. The shape of the graph indicates the optical resolution sensitivity to using several tags.

3.3 Optical FRAME: Retagging

Optical FRAME has the potential to add new techniques when used in conjunction with digital FRAME with the goal to optimise the spatial resolution and increase the image quality of the final images. Its unique techniques of retagging is investigated in this section and done so in the context of capturing images of an object at different times. Optical FRAME is utilised to re-tag the beam while digital FRAME decodes these new tags to gain the temporal resolution. Both of these objectives can be achieved in the same setup as shown in figure 11.

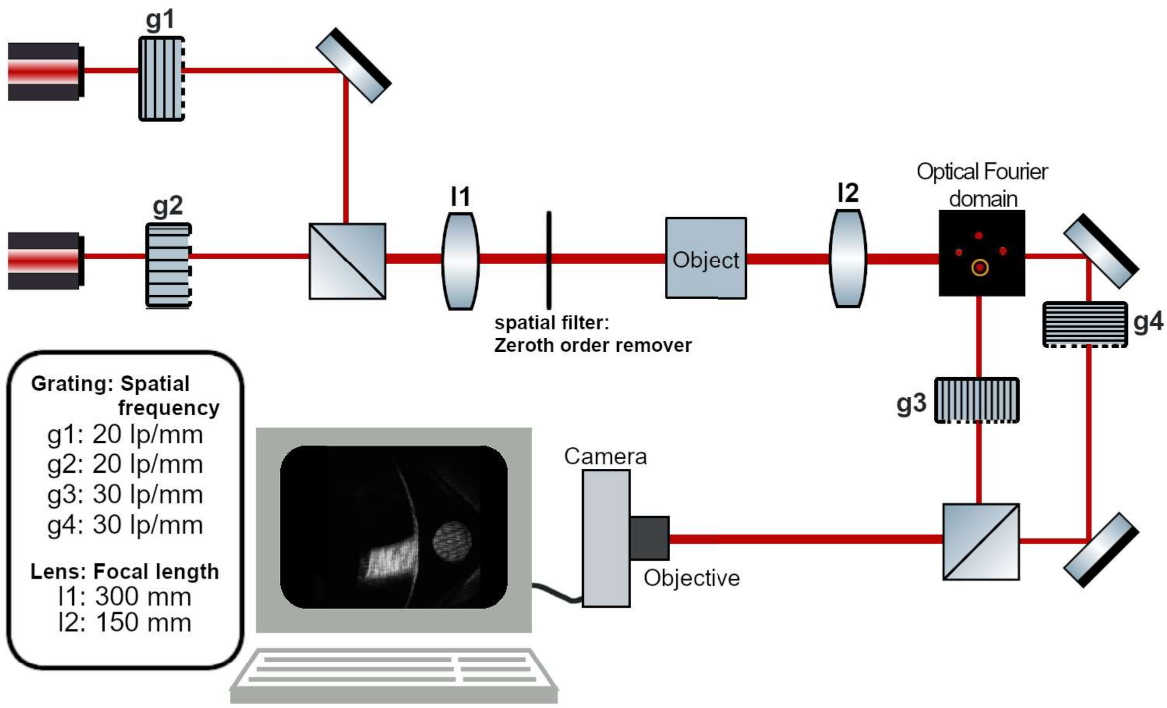

Figure 11: Schematics of the setup used for investigating optical FRAME's unique properties. The beam's are initially tagged via a grating which then goes on the illuminate the object. By isolating the necessary Fourier points in the Fourier domain they can be retagged with higher frequency gratings. The combined beam's illumination is then captured on the camera. Note that the Fourier points are isolated in the Fourier domain using the edge of a mirror to divert the paths of the beam to the necessary location.

Two lasers are pulsed at different times and are tagged with unique spatial modulations to gain information about the temporal dimension. Optical FRAME can be executed as the spatial modulations give the pulses a unique mapping in the optical Fourier domain. This allows the first orders of the unique spatial modulations to be separated. As the individual first orders contain no spatial modulation they can be re-tagged accordingly, thus performing optical FRAME to change the tag within the setup. These new tags are decoded using digital FRAME and the two images of the object at different times can be observed. The object in question is a small fan.

4 Results

This section presents and discusses the experimental work produced in this thesis.

4.1 Optical and Digital FRAME comparison

The results for the comparison between the spatial frequency limit and the intensities are shown below.

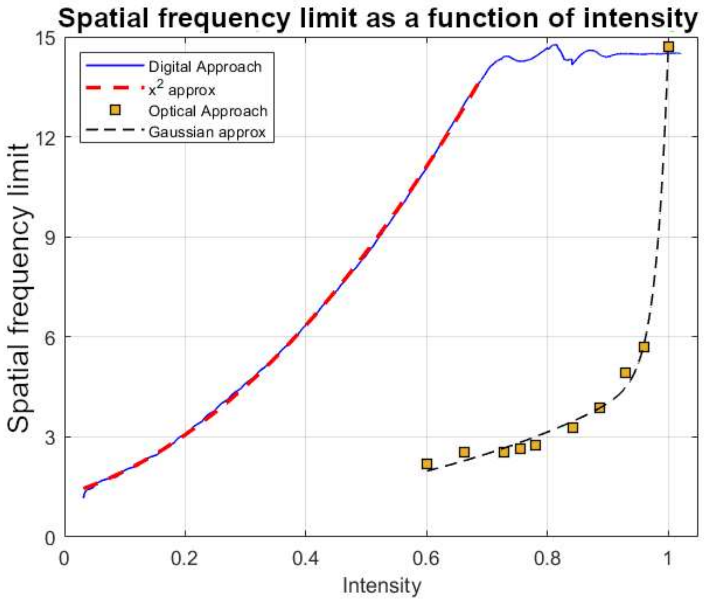

Figure 12: Graph showing the spatial frequency limit as a function of filter size (proportional to intensity) for the Optical and Digital approaches. The two curves are approximated to two functions: Digital to x^2 and Optical to e^{-x^2} (a Gaussian).

From these results several key conclusions can be drawn by contrasting the shape of the graphs. Firstly, the graphs indicate the spatial frequency distribution in the corresponding Fourier domain (optical or digital). This becomes important when utilising the approaches as high spatial frequencies in the optical approach are lost almost instantaneously when isolating the Fourier point. However at lower frequencies the rate at which the spatial frequencies are lost becomes lower than the digital counterpart. This allows optical FRAME to be used with similar results as digital FRAME when the spatial resolution required is around 3 lines/mm (spatial frequency limit).

Another curious element of the results is that the shape of the graphs are approximated to vastly different functions. This is intriguing as both approaches are seemingly doing the same thing, taking the Fourier transform of the incoming beam of light. Assuming nothing drastic occurred to the beam between the optical Fourier domain and the camera lens, the most likely explanation is a fundamental difference in how the approaches execute the Fourier transform. To further understand the differences, both the digital and optical Fourier domains are investigated.

4.1.1 Digital Fourier domain

The shape of the digital Fourier domain is dependent on the received image's spatial intensity distribution. The setup as described in figure 9 cuts the beam profile using an iris right after the beam has been expanded in an attempt to uniformly illuminate the star target image. However, doing so discards the outer parts of the beam profile. This can be seen in figure 13 a).

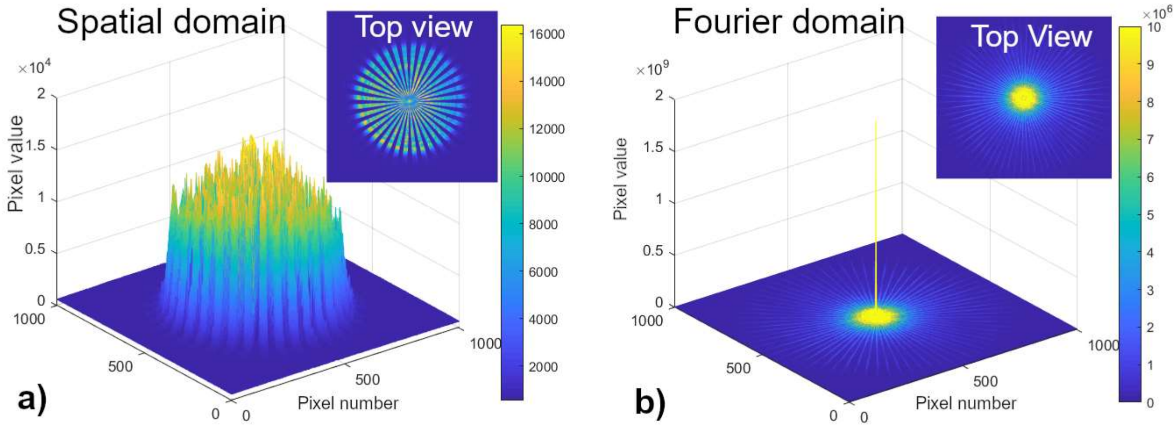

Figure 13: a) The spatial domain (as seen by the camera) with corresponding intensities and its top down view. Taking the Fourier transform gives the Fourier domain image b)

Here it is clear that the intensities of the star target represent a cylindrically symmetric top-hat step function. However, the lid of the function is curved. Given that the beam's profile is Gaussian, a likely explanation is that the function has a Gaussian lid.

By taking the Fourier transform of the entire function shown in figure 13 b) (a zoomed in version is shown below in figure 14), it is possible to see that the shape is similar to a Bessel function of the first kind. This is significant as the Fourier transform of a cynlindrically symmetric top hat is a Bessel function, suggesting that the shape of the Fourier domain is directly impacted by the shape profile of the image received. This seems to imply that the nature of the beam profile has a direct impact on the distribution of spatial frequency intensities. To further examine this hypothesis, the Fourier domain must be explored further.

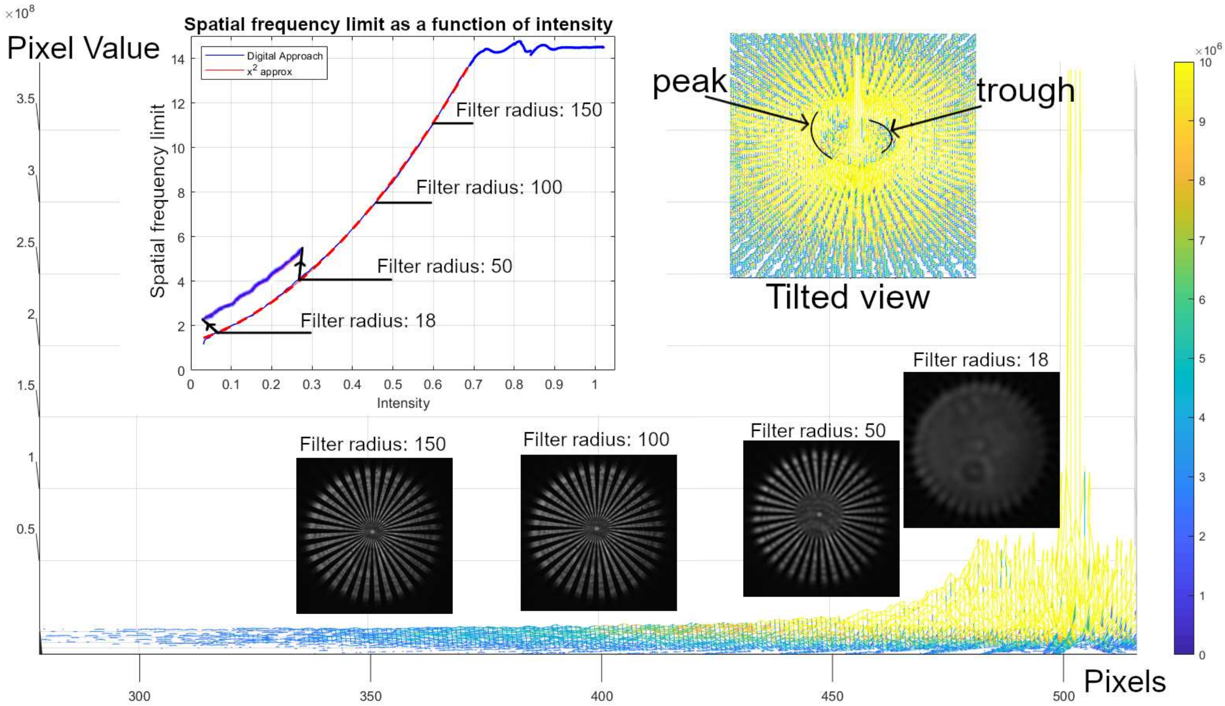

Figure 14: Zoomed in cross section of the digital Fourier domain with corresponding star target at different filter radius.

In the zoomed in Fourier domain it is possible to note a few key features. This cross section clearly has a high intensity centre which is surrounded by a symmetric peak, similar to a Bessel function of the first kind. Further examinations displays smaller oscillations beyond the surrounding peak. These oscillations can also be seen in figure 12 for the digital intensity (although are very slight) or in figure 14 between Filter radius 18 - 50 on the spatial frequency limit graph.

There could be several reasons for this distribution of spatial frequency in the Fourier domain although none are conclusive. The spatial frequency distribution as shown in figure 14 may be approximated to a linear distribution when away from the centre peak. As the filters applied are circular, decreasing the radius of the filter would create an x^2 dependence between the spatial frequencies and the intensity. The oscillations in the x^2 dependence may be the result of the Bessel functions oscillations, becoming more extreme with smaller filters.

A qualitative understanding of the spatial frequency distribution in the Fourier domain can be achieved by examining the images in figure 14. The maximum radius applied to the Fourier domain is 500 pixels (thus containing the entire Fourier domain). However, the reduction in spatial frequencies begins at a radius of 200 pixels. This gives an some intuition on the shape of the spatial frequencies as a function. Also, the reduction of spatial frequencies generally occurs away from the centre peaks. This could lead to a defining factor in the shape of the final spatial frequency limit graph.

This may be understood by acknowledging the Taylor expansion of a similar function to the cylindrically symmetric tophat. The Fourier transform of a 1 dimensional tophat function is the sinc function which, if taylor expanded, gives an x^2 dependence. As previously mentioned, the filters are applied away from the centre peak, which is where the x^2 factor dominates in the sinc function. The oscillations in the digital part of figure 12 may come from interference from the higher orders in the Taylor-expansion. However, as shown in figure 13 a), the distribution has a Gaussian lid and therefore does not have the exact properties of a tophat. The fluctuation then may occur due to the mixing of the functions.

Overall the distribution has an x^2 dependence though the reasoning is not completely understood. Variables such as the incoming beam profile seem to dictate the spatial frequency distribution. However, this experiment is performed over a star target which has a large range of distinct frequencies. Other images may not have such a distribution and thus the Fourier domain may have a different spatial frequency distributions and therefore not have as clear x^2 dependence. More investigation onto the nature of the spatial frequency distribution for different beam profiles and images is therefore required for a generalised result.

Further issues with gathering data come from the potential misalignment of the star target. Idealistically, the digital intensity graph in figure 12 should plateau at the higher spatial frequency limit. However, as the figure shows there are some fluctuations in the spatial frequency limit. Studying the MTF application's graphs suggest a slight misalignment of the star target creating aberrations in the image and thus these fluctuations. However, this effect only occurs at higher spatial frequency limits and should not impact the conclusions made in this section.

4.1.2 Optical Fourier domain

The optical frequency distribution in the Fourier domain is clearly a Gaussian distribution as seen in the optical intensity in figure 12. Taking the inverse Fourier transform allows investigation into the beam prior to the lens. A inverse Fourier transform of a Gaussian will give back itself with a different full width half maximum (FWHM). While intuitively this may makes sense as the beam is Gaussian in nature, as previously described, the beam is cut off using an iris thus changing the distribution of the beam. To further investigate this discrepancy one must understand how the locations of the spatial frequencies are distributed throughout the optical Fourier domain.

As the optical Fourier domain is not as easily examined, one can use the obtained data to suggest how the spatial frequencies are distributed. A qualitative understanding of which frequencies are lost can be obtained by comparing the different data points.

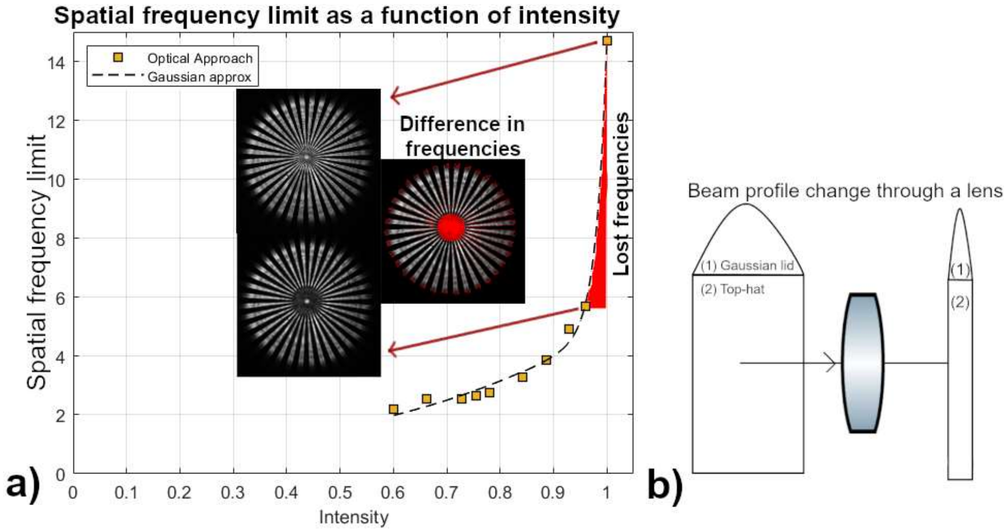

Figure 15: a) Optical spatial frequency limit to intensity comparison between data points. **b)** Top-hat with Gaussian lid being focused in a lens to produce a Gaussian-like distribution

The initial loss in spatial frequency limit indicates that many high spatial frequencies of the star target lie in outer region of the Gaussian as show in figure 15 a). The high frequencies of the star target are on the hard edges as well as in its centre. The reduction in iris size results in a drastic loss in high spatial frequencies. This results agrees with our current understanding of frequency distribution in the Fourier domain i.e. higher frequencies are further out in the Fourier domain. However, it is still unclear why the distribution in the Fourier domain behaves as a Gaussian. As previously discussed, the beam profile is more likely a circular top-hat function with a Gaussian lid as suggested by figure 13 a). Discussed below are two possible contributions to the Gaussian beam profile seen in the Fourier domain.

By considering the cylindrically symmetric top-hat with a Gaussian lid profile as two distinct function, shown in figure 15 b), one could imagine the functions being focused. This would change how they look individually but the beam profile in the optical Fourier domain may appear to be more Gaussian-like. The steep sides of the the focused Gaussian lid become akin to the top-hat functions sides. This phenomenon could potentially create a Gaussian-like function which in turn could explain the spatial frequency distribution in the optical Fourier domain.

Another possible explanation for the Gaussian approximation may be as a result of diffraction from the initial iris. The resultant diffraction pattern in the focal point is a high intensity centre region surrounded by rings of decreasing intensity, this is known as the Airy disc [8]. An intuitive perspective on how this diffraction pattern arises can be understood by taking the Fourier transform of the cylindrically symmetric top-hat function. The resulting function in an idealistic case is a Bessel function of the first kind. However, the beam width supplies a limiting factor to the shape of the beam profile in the optical Fourier domain. Therefore it may be possible that the beam profile is a Bessel function of the first kind but due to the physical limitation of the beam width, the centre peak is forced to be much larger than the idealistic case. By ignoring the relatively low intensity outer rings of the Bessel function the Airy disc can be approximated to a Gaussian distribution. This inner peak is where the filters are applied in the Fourier domain. It may be possible to observe this transformation in the optical setup but would require more intensity sensitive equipment.

While further research is required to conclusively demonstrate why the distribution of spatial frequency in the optical Fourier domain behaves similar to a Gaussian function, the presented data in figure 12 confirms that this relationship exists and defines the optical resolution of the technique.

4.2 Concluding remarks

The change in optical resolution of each technique is dependent on the shape of the spatial frequency distribution. Experimental results confirm a distinct difference in the shape of the Fourier domain depending on the method in which the Fourier domain is accessed. This may cause issues when performing optical FRAME. As higher spatial frequencies are concentrated at the edge of the Gaussian, it may result in an unavoidable reduction in spatial resolution. On the other hand, lower frequencies are lost at a slower rate than the digital counterpart. As previous experiments utilising digital FRAME have a low spatial resolution of around 3 lines/mm [9], optical FRAME may be useful in the same experimental setups as digital FRAME. Another possible benefit to optical FRAME is that the shape of the optical Fourier domain seems to have a large dependency on the optical setup. The dependency on the optical setup is also investigated in the next experiment.

However this conclusion depends on the validity of the graphs and their approximations. It seems likely however that both shapes are variants of the Bessel function of the first kind. The defining difference between the final distribution being down to how the Fourier transform is performed. Therefore, the main difference between the approaches might be that fact that they are applying filters to different parts of the same kind of Bessel function. Further investigation into the components which dictate the shape of the Fourier domain is required to fully understand how the approximation arose and what factors influence their shapes.

4.3 Proof of Concept: Simultaneous tagging

To demonstrate that the relationship described in the previous experiment holds in more complex setups, a new experiment is derived. Creating the setup illustrated in figure 10 allows for two unique spatial frequencies to tag two different images (a star target and a circular target). By isolating a first order Fourier point the camera can detect either of the images. However, as there are more tags, isolating the desired Fourier point may become more difficult due to leakage of spatial frequencies from other Fourier points. The extent to which this impacts optical FRAME's spatial frequency distribution is also investigated.

The spatial frequency limit to intensity was then obtained in much the same way as the previous experiment and the star target spatial frequency limit's are scaled to fit the previous data. It is important to note that the images related to the graphs are of the maximum spatial frequency limit for the isolated Fourier point.

4.3.1 Test 1: Full Fourier domain

The first test is taken over the entire of the Fourier domain and isolates one of the first order Fourier points. Below are the results for the experiment.

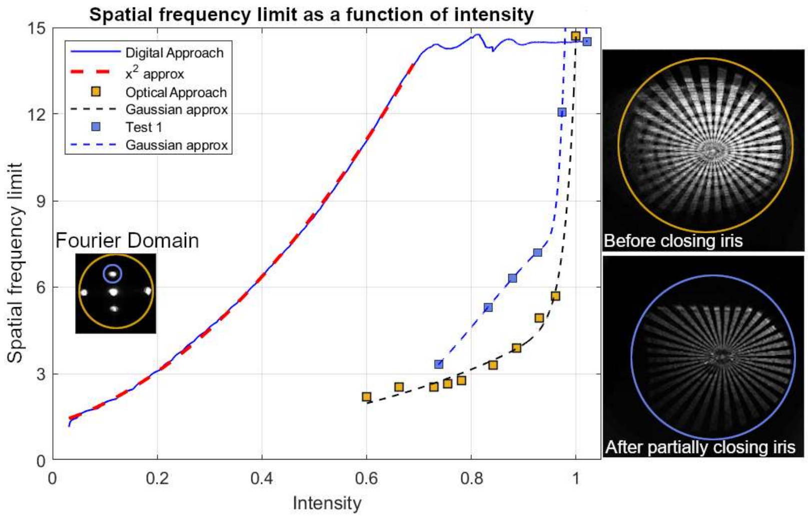

Figure 16: Spatial frequency limit to intensity graph for two tags without previously filtering the Fourier points

The graph shows two overlaying images with the unique spatial frequency (tag) visible when the iris is fully open. After partially closing the iris and isolating the desired Fourier point, only the star target with no spatial frequency is visible. This qualitative demonstration shows that optical FRAME can be performed in more complex scenarios.

While the Gaussian approximation still holds, the graph's shape is substantially different from the previous experiment's Gaussian approximation. This is thought to be due to interference with the zeroth order Fourier point. When closing the iris, the zeroth order frequencies may leak through the iris thus interfering with the spatial frequency limit final results. To avoid this, another test was performed with the zeroth order removed in a previous Fourier domain in the setup.

4.3.2 Test 2: Zeroth order removed

As the zeroth order has the largest intensity of the Fourier points, removing it reduces the chance of interference from other Fourier points leaking through the iris.

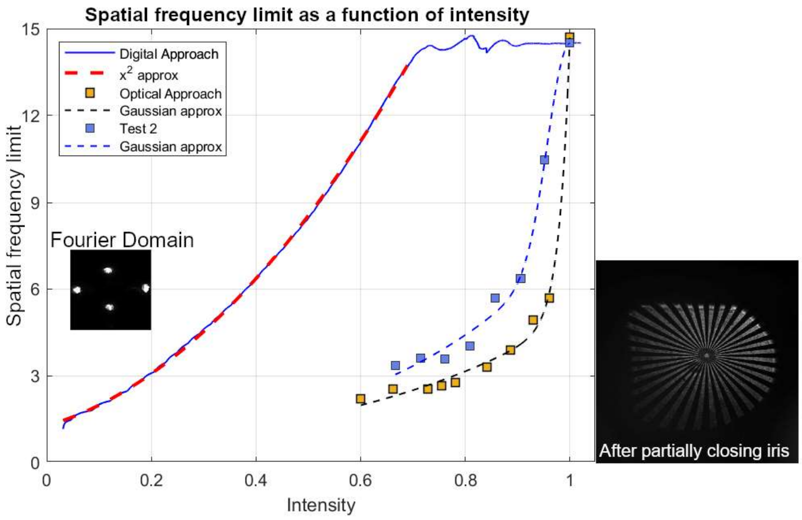

Figure 17: Spatial frequency limit to intensity graph for two tags with previous filtering of the zeroth in the Fourier domain

The graph clearly shows a Gaussian distribution and the shape is similar to the previous data. Therefore, when performing optical FRAME the zeroth order should be removed prior to isolation. Qualitatively examining the spiral image when the iris is partially closed between figure 16 and 17, one can observe that the zeroth order leaks the circular image into the centre of the star target. With this in mind, a further suggestion that other Fourier points may be influencing the spatial frequency distribution was tested.

4.3.3 Test 3: Single Fourier point

To only see the frequency distribution in the first order Fourier point of interest, all other points are removed via spatial filters.

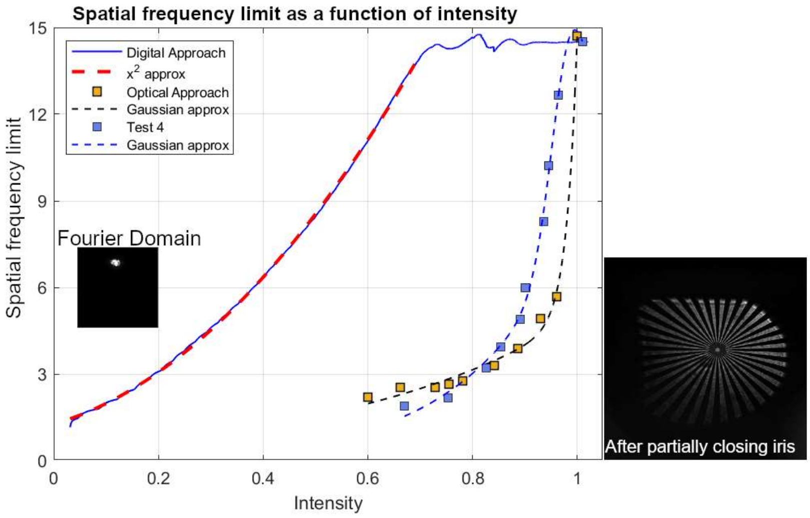

Figure 18: Spatial frequency limit to intensity graph for two tags with previous filtering of the zeroth and first orders in the Fourier domain

The data is clearly a Gaussian approximation, confirming that the Fourier points have a Gaussian distribution when the setup is made to be more complex. However, the shape of the Gaussian approximation is different than the initial comparative experiment. One suggestion for the difference in shape is due to the change in effective focal length between the first experiment and this one. The combination of lenses in the experiment resulted in a longer effective focal length. Due to this, the beam width will be larger as shown in the equation 1 below.

$$W' = \frac{\lambda}{\pi W} \cdot f \tag{1}$$

Where W' is the new beam width, W is the old beam width, λ is the wavelength of light and f is the effective focus point [6].

Therefore, the spatial frequency distribution is impacted by the strength of the effective focal length of the setup. This may add some limiters to the size as a smaller setup forces the Fourier points closer together as well as reducing the size of the spatial frequency distribution by tightening the shape of the Gaussian. On the other hand, given that the optical setup has a direct impact on the spatial frequency distribution, one can utilise this phenomena to precisely control the shape of the Gaussian. Having a weaker effective focal length creates a wider Gaussian allowing for greater control on which spatial frequencies pass through the setup. Therefore, depending on the object or experiment in which this method is being used, the spatial frequency distribution can be optimised to allow for the maximal optical resolution of the setup.

4.4 Concluding remarks

This experiment demonstrates that optical FRAME can simultaneously tag the beam to include several unique spatial frequencies without compromising the technique. Thus optical FRAME can be used for similar circumstances as digital FRAME.

Although, some precautions must be taken to remove the zeroth order Fourier point to reduce its influence on the isolated point. While this is conclusively true for impact of the zeroth order, the same can not be said for the impact of other first orders. No qualitative argument can be made for the difference in spatial frequencies distribution between test 2 and 3. Also, test 3 was performed a few days later than test 1 and 2. While this should not impact the results, slight changes in the setup may have large influence on the final result and could be a reason for the difference in Gaussian shape shown in figure 17 and figure 18.

The experiment also confirmed that the spatial frequency distribution of the Fourier point is influenced not only by the beam profile, but also the strength of the lens used to access the Fourier domain. While this may prove a challenge when working in a tight setup, if the size of the setup can be expanded, the apparatus can be chosen to optimise the optical resolution of the setup and thus the spatial resolution of the final image.

4.5 Temporally resolved imaging using optical retagging

The concept of optical FRAME has not only been shown to work, but also to be scaled to contain multiple tags. Now, the final experiment examines unique aspects of optical FRAME to be utilised either by itself, or in conjunction with digital FRAME to optimise the spatial resolution of the final images. This is examined in the context of using digital FRAME to increase the temporal resolution of the setup. Following the setup in figure 11, the temporal resolution is increased by tagging two lasers pulsed at different times and decoding the tag in post-processing. Thus in every exposure, two images are obtained. As mentioned in the method, the observed object is a small fan.

However, accessing the Fourier domain allows each "copy" of the image to be isolated. These image "copies" can now be retagged with another unique code such that digital FRAME can be performed. The proof of concept results are found below.

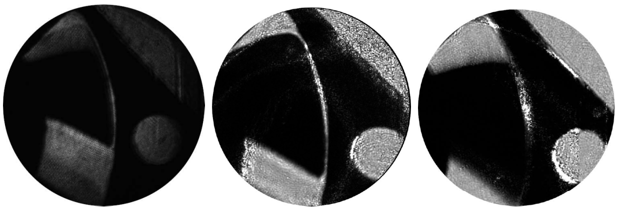

Figure 19: The raw image (left) contains two unique tags gained from retagging which can be decoded into two images of a fan taken in a single exposure 104.5 μs apart

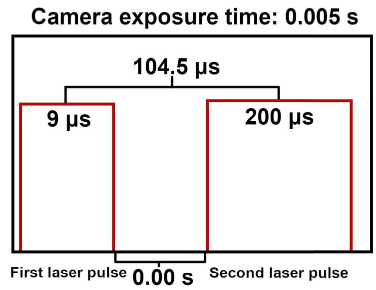

Figure 20: Time diagram for the two images collected with no delay between pulses

Figure 21: The raw image (left) contains two unique tags gained from retagging which can be decoded into two images of a fan taken in a single exposure 354.5 μs apart

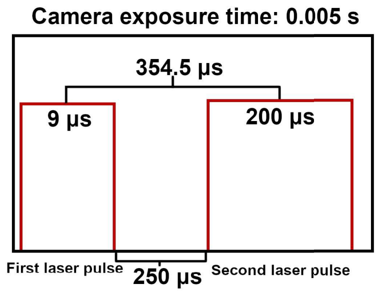

Figure 22: Time diagram for the two images collected with 250 microsecond delay between pulses

The above figures demonstrate the possibility to keep the temporal resolution whilst retagging the beam. This retagging technique is unique to optical FRAME and has the potential to increase the spatial resolution and image quality when used in conjunction with digital FRAME. To understand how this development occurs one must consider the upper limits to digital FRAME.

When capturing large quantities of images in an exposure it creates a high density of Fourier points in the digital Fourier domain. The high density as well as the zeroth order reduces the maximum size of a filter and thus reduces the spatial resolution of the final image. Although the maximal spatial resolution is set by the initial tag (due to spacing in the Fourier domain), retagging these Fourier points with a higher spatial frequency can optimise the spacing in the Fourier domain to achieve the optimal filter size and therefore improve the spatial resolution of the final images. This becomes notably important if the object is turbulent. Higher frequency structures in the wavefront are significantly influenced by refraction in turbulent media. This impact reduces the quality of the image. Therefore it becomes optimal to use lower spatial frequency tags in these turbulent samples. However, as previously described, using lower frequencies becomes an issue when there is a high Fourier point density. By retagging from a low to high spatial frequency after passing through the problematic medium, one can avoid the aforementioned trade-off between spatial resolution and image quality, thus improving the versatility of FRAME.

4.6 Increased spatial resolution using optical retagging

To quantify the retagging process one can observe how retagging can optimise the Fourier domain to increase the final images spatial resolution when compared to an image that is has not been retagged as shown in figure 23 below

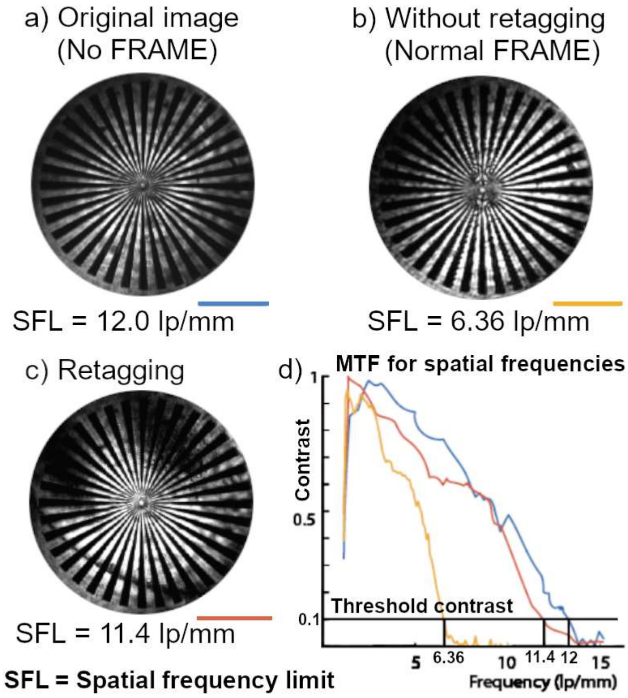

Figure 23: Three distinct images showing different spatial resolution due to differences in the optical setup. Image a) is the illumination of the star target. Image b) shows the star target with corresponding spatial frequency limit when utilising FRAME with digital filtering. Finally, Image c) demonstrates an increase in spatial resolution when performing the retagging technique. The spatial frequencies for each image can be found in the graph d)

Retagging has nearly doubled the final image's spatial frequency limit, clearly demonstrating the use of retagging to optimise the spatial resolution, even in non-turbulent samples. Optimising the spatial resolution of the final image's is vitally important to FRAME. As FRAME uses the spatial dimension as a tag, optimising the technique reduces the amount of spatial resolution that each tag "costs", while still increasing the resolution in the chosen dimension. Thus, not only will this allow FRAME to exceed its current limitations, but also potentially outperform its previous achievements.

5 Conclusion

All in all this thesis demonstrates the working operation of optical FRAME can be added to the arsenal of methods for ultra-fast imaging. Optical FRAME is capable of being used in similar applications as its digital counterpart when working with lower spatial frequencies. This includes utilising multiple tags to achieve the same setup complexity as digital

FRAME. Although there is some leakage of spatial frequencies from the zeroth order to the first orders, this can be easily removed within the setup via spatial filters and therefore is not a cause for concern. Thus demonstrating the use of optical FRAME as a stand-alone approach.

When used in conjunction with the pre-existing FRAME technique, optical FRAME's unique properties of retagging can help optimise the spatial resolution of the final images. This technique shows promising results by increasing the spatial frequency limit by almost a factor of 2 when contrasting to images that are not retagged. Retagging also has useful application when investigating turbulent samples as it creates a possibility to circumvent the aforementioned trade-off issues when using higher spatial frequency tags. Hopefully, this technique continues to be utilised in experiments to push the boundaries of investigation techniques and ultra-fast imaging to the next level.

6 Outlook

This thesis demonstrates a new optical approach that can be used to obtain similar spatial resolution as its digital counterpart. However, as the optical Fourier domain is more influence by the setup there may be creative way exploit this phenomena not achieved in this report. A key difference between the two approaches is that the Gaussian approximation for the spatial frequency distribution in the optical Fourier domain is proportional to the wavelength of light used. In order to maximise the spatial resolution, the Gaussian distribution should be narrow in the optical Fourier domain but the spacing between the Fourier points wide. This allows for a large spatial filter to isolate the Fourier point without losing higher spatial frequencies. Further investigation into whether this is possible may further optimise optical FRAME's spatial resolution. However, there is not much need for optical FRAME to compete with digital FRAME. Digital FRAME is much better at managing the final images as they are stored in the computer rather than on the illumination of the beam. Therefore, the use optical FRAME as a standalone technique is very limited as once the image "copy" has been isolated, it still needs to be captured by a camera or, if there is more than one image "copy", cameras.

Further outlook of this thesis is focused on the ability to use optical FRAME along side digital FRAME to expand the versatility of FRAME as a technique. Isolating Fourier points in the Fourier domain becomes incredibly important for retagging purposes as previously discussed. Retagging can be utilised to optimise the spatial resolution of the image by a factor of 2 and have particular use when observing turbulent samples. As optimising the technique essentially reduces the amount of resolution that each tag "costs", it can potentially advance nearly all aspects of FRAME.

Overall, this thesis developed a new way of approaching FRAME to increase its versatility such that hopefully one day, it can be used in world record beating experiments and gain a closer look into the wonders of our natural world.

References

[1] Ehn A, Bood J, Li Z, Berrocal E, Aldén M, Kristensson E. FRAME: femtosecond videography for atomic and molecular dynamics. Light: Science Applications. 2017;6(9).

[2] Nakagawa K, Iwasaki A, Oishi Y, Horisaki R, Tsukamoto A, Nakamura A, et al. Sequentially timed all-optical mapping photography (STAMP). Nature Photonics. 2014 Oct;8(9):695–700.

[3] Patterns on glass or film. Data optics; 2008. Available from: `https://www.dataoptics.com/PDF/PatternsonGlassorFilm.pdf`.

[4] Gao L, Wang LV. A review of snapshot multidimensional optical imaging: Measuring photon tags in parallel. Physics Reports. 2016;616:1–37.

[5] Suret P, Randoux S. Far Field measurement in the focal plane of a lens : a cautionary note. 2013 07;.

[6] Fourier Optics. John Wiley Sons, Ltd; 2001. Available from: `https://onlinelibrary.wiley.com/doi/abs/10.1002/0471213748.ch4`.

[7] Frantz D. High Contrast Imaging Throug h Scattering Media Using Structured Illumination Fourier Filtering; 2017. Masters thesis, Lund University.

[8] Disk L, Hollows G, James N, Inc E. Limitations on Resolution and Contrast: The Airy Disk; 2020. Available from: `https://www.edmundoptics.com/knowledge-center/application-notes/imaging/limitations-on-resolution-and-contrast-the-airy-disk/`.

[9] Li Z, Borggren J, Berrocal E, Ehn A, Aldén M, Richter M, et al. Simultaneous multispectral imaging of flame species using Frequency Recognition Algorithm for Multiple Exposures (FRAME). Combustion and Flame. 2018;192:160–169.

A

Illustration of the code for the digital approach

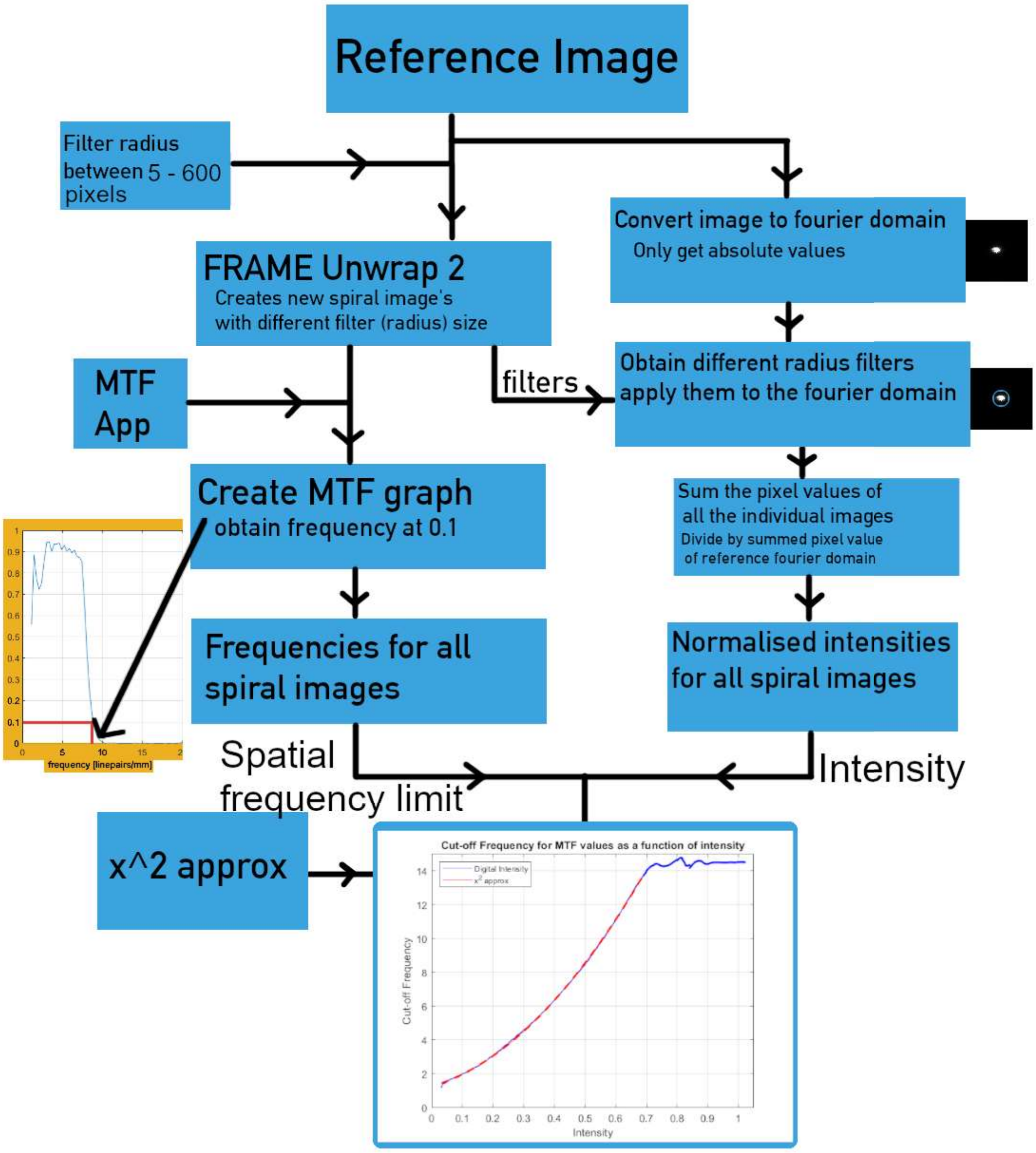

Figure 24: Data flow of code to obtain spatial frequency limit and Digital Intensity.

B

Mathematical intuition for the Fraunhoufer diffraction

To begin to understand optical Fourier transforms one can look at the beam in the far field. As shown in figure 25 , the wave front passes through a slit of size (a) and by the Huygens-Fresnel Principle [6], each point on the wave front produces a spherical wave [6].

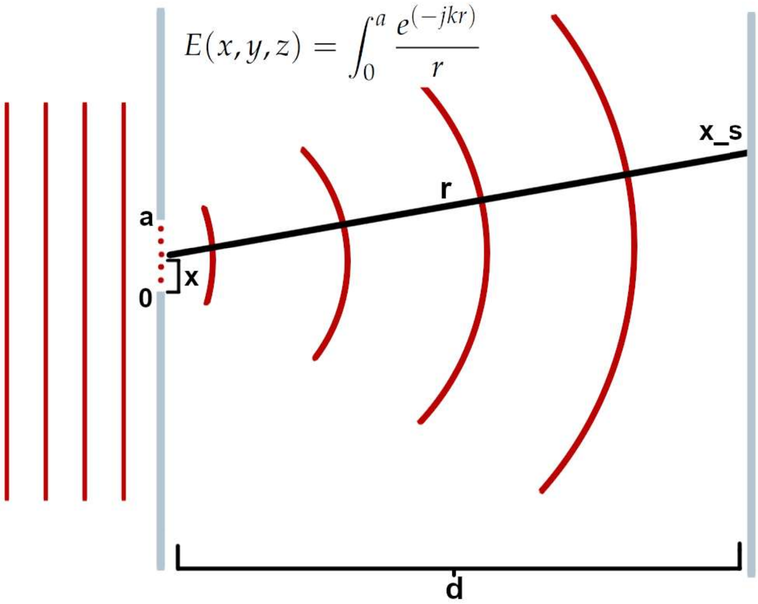

Figure 25: Illustration of a simple diffraction process.

As illustrated, the new electric field profile (E) for one point source is approximately $\frac{exp(-jkr)}{r}$ where k is the wave vector, j is the imaginary unit and r is the radial distance from the point source. By using Pythagoras theorem to substitute r, one obtains the combined electric field profile.

$$r = \sqrt{d^2 + (x_s - x)^2} \tag{2}$$

$$E = \int_0^a \frac{\exp(-jk\sqrt{d^2 + (x_s - x)^2})}{\sqrt{d^2 + (x_s - x)^2}} dx \tag{3}$$

This can be simplified by applying the Frensel approximation that $d >> x_s$ and by the same logic $d >> x$. Therefore,

$$
\begin{aligned}
r &= d\sqrt{1+\frac{(x_s-x)^2}{d^2}}, \quad (\text{Where } \frac{(x_s-x)^2}{d^2} < 1) \\
r &\approx d + \frac{(x_s-x)^2}{d}, \quad \text{as } \sqrt{1+\epsilon} \approx 1 + \frac{1}{2}\epsilon + ...
\end{aligned} \tag{4}
$$

By placing the r approximation shown in the equation above into equation 3 and simplifying.

$$
E \approx e^{-jkd} \int_0^a \frac{\exp(-jk\frac{(x_s-x)^2}{d})}{d + \frac{(x_s-x)^2}{d}} dx \tag{5}
$$

By expanding $(x_s - x)^2$ and applying the previous approximations, the x^2 term is removed as well as $\frac{(x_s-x)^2}{d}$ in the lower denominator. This is known as the Fraunhofer approximation and obtains the equations,

$$
E \approx \frac{1}{d} e^{-jkd} e^{-jk\frac{x_s^2}{2d}} \int_0^a \exp{(jkx_s x)} dx \tag{6}
$$

This derivation has used the narrow slit shown in figure 25, which limited the integral between 0 and a, similar to a tophat function. However, the shape of the function is not restricted by this derivation. Therefore one can replacethe tophat function with a universal $g(x)$, defined as the shape of the aperture.

$$
E \approx \frac{1}{d} e^{-jkd} e^{-jk\frac{x_s^2}{2d}} \int_{-\inf}^{\inf} g(x) \exp{(jkx_s x)} dx \tag{7}
$$

Finally, the small angle approximation can be utilised as the angle between the point source and the screen will be small. This defines the variable $k_x = \frac{x_s}{d} k$.

$$
E \approx \frac{1}{d} e^{-jkd} e^{-jk\frac{x_s^2}{2d}} \int_{-\inf}^{\inf} g(x) \exp{(jk_x x)} dx \tag{8}
$$

The integral shown above is the Fourier Transform of the aperture function $g(x)$. Therefore the Fourier domain can be obtained at the far-field of the system.

This is further proven by taking the intensity of the electric field as

$$
\begin{aligned}
I &= |E|^2 \\
\mathcal{F}(g(x)) &= \int_{-\inf}^{\inf} g(x) \exp{(jk_x x)} dx \\
I &= \frac{1}{d^2} |\mathcal{F}(g(x))|
\end{aligned}
\tag{9}
$$

In order for the Fourier domain to be visible, the terms outside of the integral (which impact the phase of the beam) cancel out. This process can be scaled for the y-dimensions without loss of generality, thus giving a 2D Fourier transform between spatial frequency and spatial co-ordinates in the far-field. Observing the Fourier domain in the far-field is known as Fraunhoufer diffraction.

C
Derivations

C.1 Derivation of lens equation

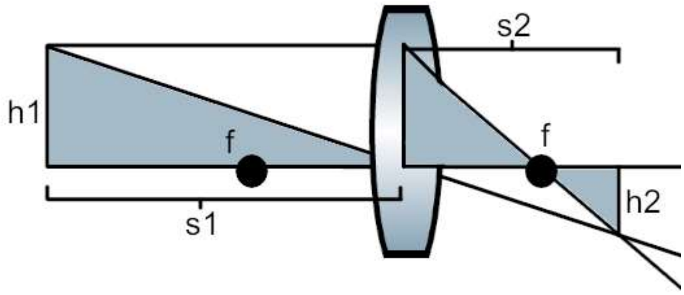

Figure 26: Illustration of a convex lens for use in the derivation of the lens equation

From figure 26 above it is possible to obtain two equations due to its geometry and utilising the thin lens approximation.

$$\frac{h1}{s1} = \frac{h2}{s2} \quad (10)$$

$$\frac{h1}{f} = \frac{h2}{s2 - f} \quad (11)$$

From here it is possible to rearrange these equations such that:

$$\frac{h1}{h2} = \frac{s1}{s2} = \frac{f}{s2 - f} \quad (12)$$

$$f = \frac{s1s2}{s1 + s2} \quad (13)$$

$$\frac{1}{f} = \frac{1}{s1} + \frac{1}{s2} \quad (14)$$

Equation 14 is utilised in experiments as a guide for finding the focal point for a single lens.

C.2 Derivation of the back focal length equation

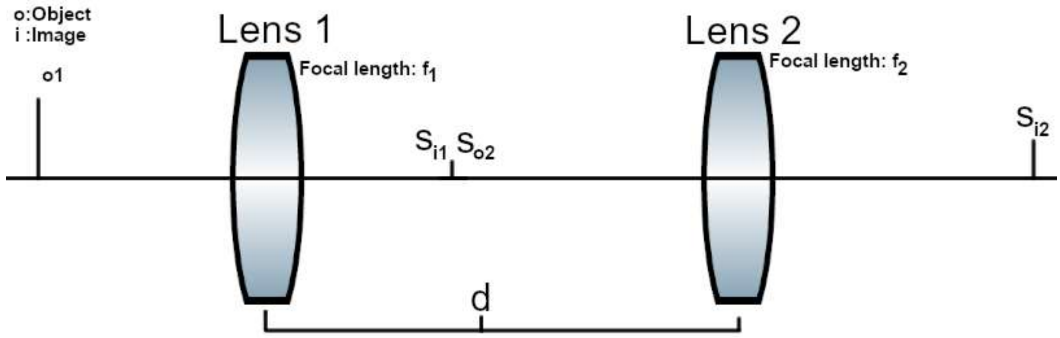

Figure 27: Illustration of a two lenses used to derive the back focal length equation

The back focal length of a system of two lenses can be derived using the a simple relation shown in figure 27.

$$s_{o2} = d - s_{i1} \tag{15}$$

Now, using the lens equation derived in the previous section, s_{i2} can be described as a function of the incoming light, the distance between the lenses and their corresponding focal lengths. To do so

$$s_{i1} = \frac{f_1 s_{o1}}{s_{o1} f_1}, \qquad s_{i2} = \frac{f_2 s_{o2}}{s_{o2} - f_2} \tag{16}$$

Combining equations 16 and 15 gives the result.

$$s_{i2} = \frac{f_2 (d - \frac{f_1 s_{o1}}{s_{o1} - f_1})}{d - f_2 - \frac{f_1 s_{o1}}{s_{o1} - f_1}} \tag{17}$$

Now the two lens setup can be described only by the incoming rays. If these rays are parallel, the resultant image will be at the effective focal length of the setup (the two lenses). Parallel rays implies that $s_{o1} \rightarrow \inf$ or $\frac{1}{s_{o1}} \rightarrow 0$. Applying this to equation 17 gives the back focal length (the distance from the last lens to the focal point).

$$\text{BFL} = \frac{f_2 d - f_1}{d - (f_1 + f_2)} \tag{18}$$

Equation 18 is used as a guide to find the Fourier domain for systems with 2 lenses (The maximum used in this report).